JCTC Journal of Chemical Theory and Computation

Article

pubs.acs.org/JCTC

Improving the Accuracy of Excited-State Simulations of BODIPY and Aza-BODIPY Dyes with a Joint SOS-CIS(D) and TD-DFT Approach

Siwar Chibani,[†] Adèle D. Laurent,*[,†] Boris Le Guennic,*[,‡] and Denis Jacquemin*[,†,§]

[†]Laboratoire CEISAM - UMR CNRS 6230, Université de Nantes, 2 Rue de la Houssinière, BP 92208, 44322 Nantes Cedex 3, France

[‡]Institut des Sciences Chimiques de Rennes, UMR 6226, CNRS-Université de Rennes 1, 263 Av. du General Leclerc, 35042 Rennes Cedex, France

[§]Institut Universitaire de France, 103 bd Saint-Michel, F-75005 Paris Cedex 05, France

Supporting Information

ABSTRACT: BODIPY and aza-BODIPY dyes constitute two key families of organic dyes with applications in both materials science and biology. Previous attempts aiming to obtain accurate theoretical estimates of their optical properties, and in particular of their 0−0 energies, have failed. Here, using time-dependent density functional theory (TD-DFT), configuration interaction singles with a double correction [CIS(D)], and its scaled-opposite-spin variant [SOS-CIS(D)], we have determined the 0−0 energies as well as the vibronic shapes of both the absorption and emission bands of a large set of fluoroborates. Indeed, we have selected 47 BODIPY and 4 aza-BODIPY dyes presenting diverse chemical structures. TD-DFT yields a rather large mean signed error between the experimental and theoretical 0−0 energies with a systematic overshooting of the transition energies (by ca. 0.4 eV). This error is reduced to ca. 0.2 [0.1] eV when the TD-DFT 0−0 energies are corrected with vertical CIS(D) [SOS-CIS(D)] energies. For BODIPY and aza-BODIPY dyes, both CIS(D) and SOS-CIS(D) clearly outperform TD-DFT. The present computational protocol allows accurate data to be obtained for the most relevant properties, that is, 0−0 energies and optical band shapes.

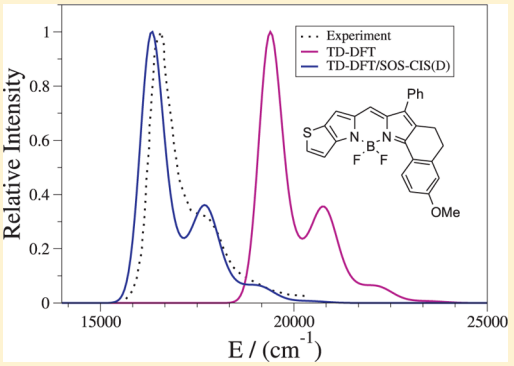

1. INTRODUCTION

Near-infrared (NIR) dyes, which present absorption and emission wavelengths between 700 and 1700 nm, are of crucial importance for several applications, e.g., photovoltaics,[1,2] advanced optoelectronics,[3−5] nonlinear optics,[6−8] bioimaging or sensing,[9−12] and photodynamic therapy.[13−15] Among the various NIR dyes, boron-dipyrromethene (BODIPY) derivatives and their nitrogenated parents, aza-boron-dipyrromethene (aza-BODIPY) dyes, probably constitute the two most developed families. The success of BODIPY and aza-BODIPY derivatives is due to their remarkable photophysical properties, starting with large molar absorption coefficients, high fluorescence quantum yields, NIR emission and going to superior photostabilities in both solution and solid state.[16−18]

Simulation of the electronically excited state (ES) properties of both BODIPY and aza-BODIPY, which can be viewed as *cis*-constrained cyanines, is a significant challenge for quantum-mechanical methods because of the well-documented *cyanine challenge*: the differential electron correlation effects are difficult to capture in these compounds.[19−22] Several studies have focused on comparisons between experimental and theoretical data for (aza-)BODIPY derivatives using the vertical approximation.[23−37] This approach simply consists of single-point ES calculations performed on the optimal geometry of the ground state (GS). However, this approximation is not suitable to mimic measured optical spectra as it does not allow well-grounded comparisons with experiments. To access such comparisons, one needs to compute the vibronic structures of the absorption and emission bands or/and the 0−0 energies (E^{0-0}). We have previously performed such investigations for both aza-BODIPY and BODIPY dyes.[38,39] In order to determine the 0−0 energies, the GS and ES structures should be optimized and the vibrational frequencies of both states should also be determined. As a result of the implementation of analytical ES derivatives, time-dependent density functional theory (TD-DFT) has emerged as the most convenient theory to perform these tasks.[40] TD-DFT successfully restores several key features of aza-BODIPY and BODIPY: (1) the band shapes of dyes presenting significant vibronic coupling; (2) the solvatochromic effects; (3) the relative charge transfer (CT) character of different states; (4) the impact of auxochromes on the evolution of the experimental 0−0 energies (the meeting point between absorption and fluorescent curves, AFCP).[38,39] Despite these successes, a serious drawback has appeared: the TD-DFT transition energies are overestimated with very large mean signed errors (MSEs), e.g., 0.4 eV for BODIPY dyes.[39] This is in the line of previous results to model cyanine chains.[19−21,41,42] Therefore, an apparent deadlock has been reached, as on the one hand TD-DFT is not very accurate for

Received: July 23, 2014
Published: August 29, 2014

   dx.doi.org/10.1021/ct500655k | *J. Chem. Theory Comput.* 2014, 10, 4574−4582

Scheme 1. Representation of the First Series of BODIPY Dyes Investigated Here[a]

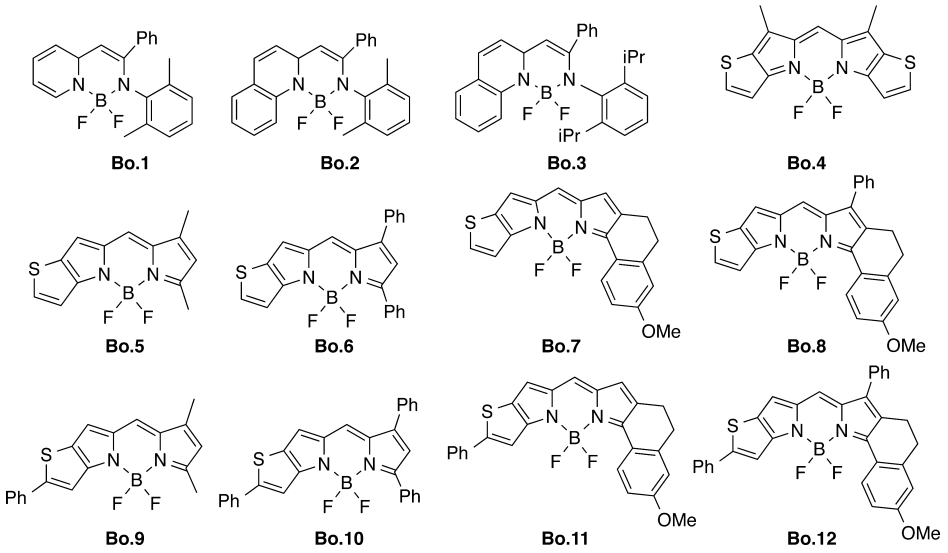

[a]The measured longest wavelength of absorption (λ_{abs}), emission wavelength (λ_{emi}), and solvents used as well as the experimental references can be found in Table S-I in the Supporting Information (SI).

Scheme 2. Representation of the Aza-BODIPY Dyes Investigated Here[a]

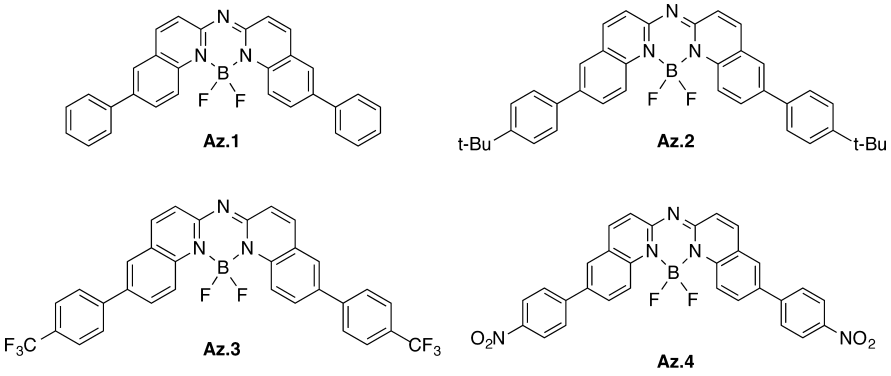

[a]The experimental data and references can be found in Table S-II in the SI.

these dyes, but on the other hand, theoretical schemes that are efficient for cyanines (e.g., CC3 or GW-BSE) do not allow analytic ES optimization,[41,42] and their use to obtain the 0−0 energies of *real-life* BODIPY is very difficult because of their computational requirements. For this reason, the present work proposes the use of an alternative approach combining TD-DFT and configuration interaction singles with a double correction [CIS(D)], which are approaches for determining structures and transition energies, respectively. CIS(D), developed by Head-Gordon and co-workers,[43,44] is one of the most adequate method to describe transition energies in organic and inorganic molecules.[45,46] In CIS(D), dynamic electron correlation is introduced via double substitutions, and it can be considered as an ES analogue of the GS second-order Møller−Plesset theory (MP2) approach.[43,44] Comparisons of the performances of CIS, CIS(D), and TD-DFT vertical excitation energies have already been published.[19,21,47,48] It has been shown that CIS(D) generally outperforms both CIS and TD-DFT, although the extent of the difference between CIS(D) and TD-DFT is strongly system-dependent. Interestingly, Grimme and Neese[19] and Moore and Autschbach[21] found that CIS(D) is an effective approach to model cyanines. We also note that the spin-scaled approaches derived from CIS(D) were found to be at least as powerful as the original scheme in describing ESs, although they present a reduced computational cost compared to the unscaled methods.[49−51] For instance, TD-DFT, CIS(D), and scaled-component-spin CIS(D) [SCS-CIS(D)] methods have been used to calculate gas-phase ES energies of 32 valence states presenting $\pi \rightarrow \pi^*$ or $n \rightarrow \pi^*$ character, and it was figured out that both CIS(D) and SCS-CIS(D) are more accurate than TD-DFT.[46,52] In that study, the mean absolute errors (MAEs) were around 0.2 eV for CIS(D) and SCS-CIS(D) and 0.3 eV for TD-DFT. More recently, Goerigk and Grimme[53] found that SCS-CIS(D) and scaled-opposite-spin CIS(D) [SOS-CIS(D)] yield similar results that again are superior to those obtained using the TD-DFT method for 12 molecules, including two charged species. The spin-scaled approaches can also be applied with the second-order coupled-cluster method (CC2);[54] and Winter and co-workers performed a benchmark of the 0−0 energies of 66 aromatic organic molecules in the gas phase using CC2, SCS-CC2, and SOS-CC2, and they concluded that SCS-CC2 is the most accurate approach.[55] A disadvantage of CIS(D) and its variations, however, is that they are in practice much less efficient than TD-DFT for determining ES vibrational structures and geometries. This explains why TD-DFT

dx.doi.org/10.1021/ct500655k | J. Chem. Theory Comput. 2014, 10, 4574−4582

Table 1. Statistical Analysis for the BODIPY Dyes Shown in Scheme 1 Obtained with the PCM-TDDFT, CIS(D), and SOS-CIS(D) Approaches (All Values except R^2 Are Given in eV)

method	MSE	MAE	SD	R^2	Max(+)	Max(−)
E_{BE}^{AFCP}(TD, SS, neq)	0.403	0.403	0.046	0.992	0.510	0.348
E_{BE}^{AFCP}(CIS(D), SS, neq)	0.279	0.279	0.069	0.979	0.339	0.108
E_{BE}^{AFCP}(SOS-CIS(D), SS, neq)	−0.020	0.030	0.034	0.991	0.057	−0.072

structural and vibrational data have been previously used to convert experimental 0−0 energies into vertical absorption values to allow the straightforward use of CIS(D).[53] In a similar line, the aim of the present study is to assess the performance of both the CIS(D) and SOS-CIS(D) methods in simulating the 0−0 energies of two series of BODIPY and aza-BODIPY dyes (see Schemes 1 and 2) that, as stated above, constitute strong challenges for TD-DFT. Our goal is to reduce the systematic overestimation of the experimental 0−0 energies obtained with TD-DFT by adding corrections from the CIS(D) or SOS-CIS(D) approaches. To the very best of our knowledge, no previous theoretical works using refined ab initio approaches have focused on the optical signatures of the compounds displayed in Schemes 1 and 2.

The paper is divided into four major parts. In the first and second sections, we outline the computational procedures and protocol, respectively. In the third and the fourth parts, we investigate the 0−0 energies and vibronic shapes of a large number of BODIPY and aza-BODIPY dyes using a blend of CIS(D) or SOS-CIS(D) and TD-DFT approaches.

2. COMPUTATIONAL DETAILS

DFT, TD-DFT, and CIS(D) calculations were carried out with the latest version of the Gaussian 09 program package,[56] applying both a tightened self-consistent field convergence criterion (10^{-9}−10^{-10} au) and an improved optimization threshold (10^{-5} au on average forces). The same DFT integration grid, the so-called *ultrafine* pruned (99,590) grid, was used for both the ground and excited states. All of our DFT and TD-DFT calculations were performed with the M06-2X hybrid exchange−correlation functional.[57] The choice of this functional was dictated by our previous benchmarks performed on aza-BODIPY and BODIPY dyes, which demonstrated that M06-2X provides very good consistency with experimental trends for optical spectra.[38,39] We previously investigated atomic basis set and solvent effects for both aza-BODIPY and BODIPY families and found (1) that the geometrical and vibrational parameters can be determined with the 6-31G(d) basis set using the polarizable continuum model (PCM) to account for solvent effects; (2) that the transition energies need to be corrected with a much larger atomic basis set, 6-311+G(2d,p); and (3) that state-specific[58] PCM (SS-PCM)[59] results yield consistent chemical trends when the non-equilibrium (neq) limit is considered.[38,39] Therefore, we followed these conclusions in the present work (see below). The SOS-MP2 and SOS-CIS(D) energies were determined with the Q-Chem package using the resolution of identity (RI) scheme with a double-ζ auxiliary basis set.[60]

Vibrationally resolved spectra within the harmonic approximation were computed using the FCclasses program (FC) on the basis of TD-DFT vibrational signatures.[61−64] The reported spectra were simulated using a convoluting Gaussian function presenting a half width at half-maximum (HWHM) that was adjusted to allow direct comparisons with experiments (typical value 0.04 eV). A maximal number of 25 overtones for each mode and 20 combination bands for each pair of modes were included in the calculation. The maximum number of integrals to be computed for each class was first set to 10^6. In the cases where convergence of the Franck−Condon (FC) factor (≥0.9) could not be achieved with this number of integrals, a larger value (10^{12}) was used to go over the 0.9 limit.

As stated in the Introduction, 0−0 TD-DFT calculations were corrected with transition energies obtained with CIS(D) and SOS-CIS(D) values. To simulate the AFCP energies using the TD-DFT approach, we applied our previously proposed strategy,[39,65] which is summarized in the SI. In this protocol, the best estimates (BEs) of the AFCP energies can be obtained by adding a correction for nonequilibrium effects to the equilibrium (eq) 0−0 energies:

$$E_{BE}^{AFCP}(\text{TD, SS, neq}) = E_{BE}^{0-0}(\text{TD, SS, eq}) + \frac{1}{2}[\Delta E_{neq/eq}^{vert-a}(\text{SS}) + \Delta E_{neq/eq}^{vert-f}(\text{SS})] \quad (1)$$

where the second term is defined in eqs S-5 and S-6 in the SI. The CIS(D) and SOS-CIS(D) estimates make use of the optimized geometries of the GS and ES respectively obtained by the PCM-DFT and PCM-TD-DFT approaches and consist of gas-phase single-point calculations with the 6-31G(d) atomic basis set. The adiabatic energies are expressed as follows:

$$E_{6\text{-}31G(d)}^{adia}(Y) = E_{6\text{-}31G(d)}^{ES}(Y) - E_{6\text{-}31G(d)}^{GS}(X) \quad (2)$$

where X = MP2 or SOS-MP2 and Y = CIS(D) or SOS-CIS(D). In order to obtain the AFCP energies, we use the expression

$$E_{BE}^{AFCP}(\text{Y, SS, neq}) = E_{BE}^{AFCP}(\text{TD, SS, neq}) + E_{6\text{-}31G(d)}^{adia}(Y) - E_{6\text{-}31G(d)}^{adia}(\text{TD, gas}) \quad (3)$$

where the TD-DFT adiabatic energies in the gas phase are simply given by

$$E_{6\text{-}31G(d)}^{adia}(\text{TD, gas}) = E_{6\text{-}31G(d)}^{ES}(\text{TD, gas}) - E_{6\text{-}31G(d)}^{GS}(\text{gas}) \quad (4)$$

In short, in eq 3 the structural, vibrational, basis set, and solvation effects are determined with TD-DFT whereas the vertical transition energies are computed with CIS(D) or SOS-CIS(D).

3. RESULTS AND DISCUSSION

3.1. BODIPY Dyes. *3.1.1. 0−0 Energies.* In order to determine the most efficient approach to compute the AFCP energies of the BODIPY dyes presented in Scheme 1, we compare figures obtained using TD-DFT [E_{BE}^{AFCP}(TD, SS, neq); eq 1], CIS(D) [E_{BE}^{AFCP}(CIS(D), SS, neq); eq 3], and SOS-CIS(D) [E_{BE}^{AFCP}(SOS-CIS(D), SS, neq); eq 3]. The results of a statistical analysis for these 12 molecules, including the MSEs,

dx.doi.org/10.1021/ct500655k | J. Chem. Theory Comput. 2014, 10, 4574−4582

MAEs, standard deviations (SDs), linear determination coefficient (R^2) values, and the maximal positive and negative deviations [Max(+) and Max(−)], are collected in Table 1 and a graphical comparison of the theoretical and experimental energies is given in Figure 1. The raw data obtained with TD-DFT-M06-2X, CIS(D), and SOS-CIS(D) are provided in the SI. The results in Table 1 show a significant difference among the three selected approaches. First, while TD-DFT yields the maximal value of R^2 (0.992) with a relatively small SD (0.046 eV), this success comes at the price of large MSE and MAE (0.403 eV), indicating that the experimental values are systematically overestimated, in agreement with the results of our previous BODIPY study.[39] It is worth noting that such error significantly exceeds the typical TD-DFT inaccuracy.[66] As mentioned in the Introduction, our goal is to decrease the error between the experimental and theoretical energies while conserving the high-quality correlation obtained with TD-DFT. Going from TD-DFT to CIS(D) reduces the MSE and MAE by 0.124 eV, but the value of R^2 (0.979) is slightly deteriorated compared with TD-DFT. We also note that CIS(D) provides the largest SD (0.069 eV). Interestingly, SOS-CIS(D) and TD-DFT provide very similar correlations. Indeed, for SD (R^2), we obtain 0.046 eV (0.992) and 0.034 eV (0.991) for TD-DFT and SOS-CIS(D), respectively. The difference in the R^2 values obtained with these two methods is therefore completely negligible (0.001). More importantly, we underline that SOS-CIS(D) not only gives a small negative MSE (−0.020 eV), indicating that the experimental values are on average slightly underestimated, but also yields a tiny MAE. Indeed, including the SOS-CIS(D) corrections drastically reduces the MAE by more than 1 order of magnitude (0.403 to 0.030 eV). This is in the line of the work of Grimme and Izgorodina,[46] but the improvement is much more significant here. In conclusion, the SOS-CIS(D) method clearly outperforms both TD-DFT and CIS(D) and appears to be a nearly perfect scheme to obtain the 0−0 energies of the BODIPY dyes shown in Scheme 1.

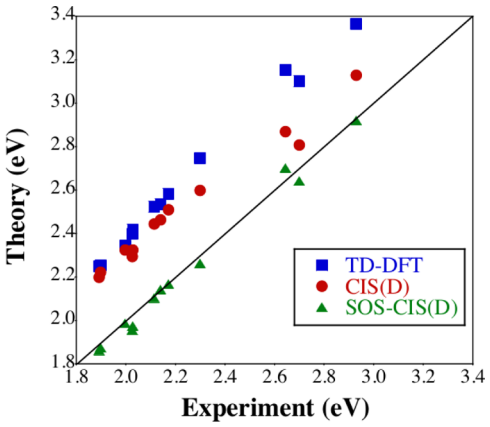

Figure 1. Comparison of the TD-DFT, CIS(D), SOS-CIS(D), and experimental E^{AFCP} values for the BODIPY dyes shown in Scheme 1.

To check that the exceptional performance of SOS-CIS(D) obtained with only 12 BODIPY dyes is not simply a lucky outcome, it was necessary to increase the chemical diversity of the set of derivatives considered. In that framework, we computed with SOS-CIS(D) the AFCP energies of 35 structurally diverse BODIPY dyes extracted from a previous TD-DFT investigation[39] (see Scheme 3). Table 2 lists the statical data obtained for this larger set of compounds (the raw data can be found in the SI). It is obvious that TD-DFT yields a small SD and large R^2 but systematically overshoots the experimental 0−0 energies by a value close to 0.4 eV. This confirms that TD-DFT approach is only *chemically accurate* for the ES energies of BODIPY dyes. On the contrary, SOS-CIS(D) yields an MAE smaller than 0.1 eV, and the difference between the R^2 values for the two approaches is again negligible (0.004). Figure 2 confirms the improvement brought by SOS-CIS(D). For the records, we have determined the MAE for the full set of 47 BODIPY dyes and we obtained 0.382 eV (TD-DFT) and 0.079 eV [SOS-CIS(D)]. We conclude that the mixed SOS-CIS(D)//TD-DFT approach proposed here, that combines TD-DFT structural and vibrational data to SOS-CIS(D) vertical energies, is extremely efficient for BODIPY dyes: it allows to attain both absolute and relative accuracies for large molecules, a feat beyond the reach of the methods taken separately.

3.1.2. Impact of the Auxochromes. Let us now turn toward a more chemical analysis. Figure 3 shows the density difference plots computed for four BODIPY dyes presenting the same core, namely, **Bo.9**, **Bo.10**, **Bo.11**, and **Bo.12** (see Scheme 1). In order to provide a more complete characterization of the ES of these compounds, we determined the CT parameters [the CT distance (d^{CT}), the transferred charge (q^{CT}), and the CT dipole moment (μ^{CT})] through Le Bahers' model,[67,68] and the results are listed in Table 3. With the SOS-CIS(D) scheme, replacing the side methyl group (**Bo.9**) by a phenyl ring (**Bo.10**) induces a bathochromic shift of +39 nm (absorption) and +48 nm (emission), auxochromic effects matching well the corresponding experimental values of +40 and +43 nm, respectively. Interestingly, going from **Bo.9** to **Bo.10** induces a decrease in the CT distance from 1.81 to 1.28 Å (Table 3). Although one could consider that the phenyl substituent acts as a secondary weak electron donor (in blue in Figure 3), this indicates that the observed bathochromic shift is not related to enhanced CT. Replacing the methyl group (**Bo.9**) by a strong anisole donor group and stiffening the dye (**Bo.11**) induces large bathochromic shifts of +94 and +63 nm for absorption and emission, respectively (the experimental values are +74 and +74 nm, respectively). We again note that the CT distance and CT dipole moment decrease in going from **Bo.9** to **Bo.11**, so the evolution of optical signatures of these compounds cannot be simply explained on the basis of the chemically intuitive CT parameters.

3.1.3. Vibronic Spectra. The simulated vibrationally resolved spectra of **Bo.5**, **Bo.6**, **Bo.7**, and **Bo.8** obtained using TD-DFT considering TD-DFT or SOS-CIS(D) 0−0 energies are displayed in the left and right panels of Figure 4. Of course, one only notices a red shift in all of the spectra with the latter scheme, as the same vibrational structures are used in the two calculations. Compared to experiment,[69] the overall position of the bands is, as expected, much more accurate with SOS-CIS(D), and the successive redshifts in the **Bo.5** → **Bo.8** series are also well-restored. It is also clear that theory reproduces the main features of the absorption and emission bands, with the presence of shoulders that are less intense for emission than for absorption.[69] In our calculations, the intensity of these shoulders is nevertheless slightly overestimated compared to experiment. To unravel the origin of these specific band shapes, we examined the individual vibronic components (Figure 5), but no specific vibrational mode particularly stands out as responsible for the presence of the shoulders.

dx.doi.org/10.1021/ct500655k | J. Chem. Theory Comput. 2014, 10, 4574−4582

Scheme 3. Representation of the Second Series of BODIPY Dyes Investigated Here[a]

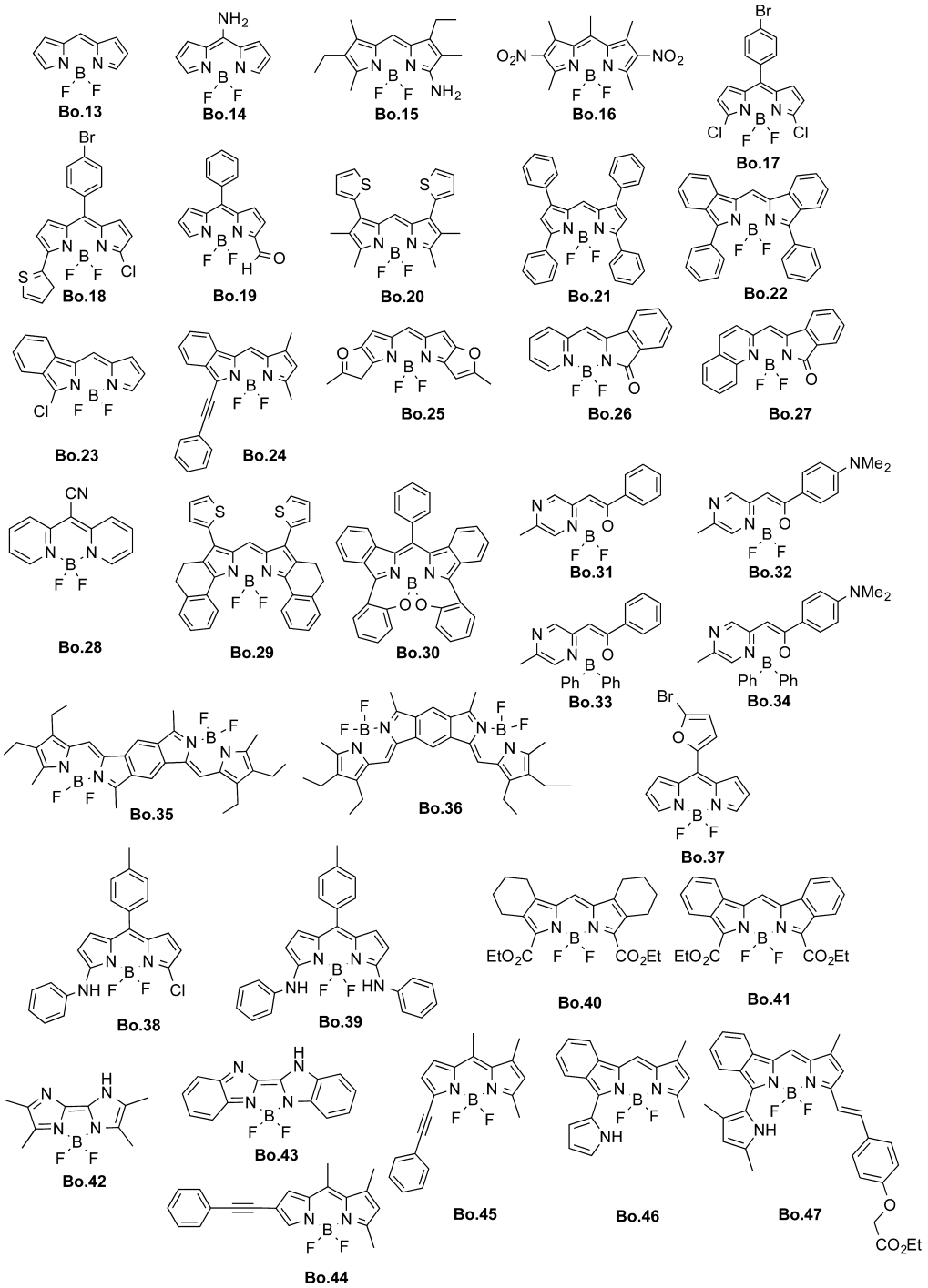

[a]These molecules were taken from ref 39, and all of the experimental data can be found in the SI of that earlier work.

Table 2. Statistical Analysis for the BODIPY Dyes Shown in Scheme 3 Obtained with the PCM-TDDFT and SOS-CIS(D) Approaches (All Values except R^2 Are Given in eV)

method	MSE	MAE	SD	R^2	Max(+)	Max(−)
E_{BE}^{AFCP}(TD, SS, neq)	0.375	0.375	0.073	0.974	0.513	0.185
E_{BE}^{AFCP}(SOS-CIS(D), SS, neq)	−0.076	0.095	0.083	0.970	0.091	−0.264

3.2. Aza-BODIPY dyes. Wang and co-workers[70] recently synthesized a new series of aza-BODIPY dyes presenting very extended π delocalization. These compounds exhibit very strong $\pi \rightarrow \pi^*$ absorption bands, intense fluorescence emissions in the visible region, and large photoluminescence quantum yields. Our aim is to observe whether the new SOS-CIS(D)//TD-DFT protocol is also efficient for this family of compounds. The statistical analysis for the four aza-BODIPY

dx.doi.org/10.1021/ct500655k | J. Chem. Theory Comput. 2014, 10, 4574−4582

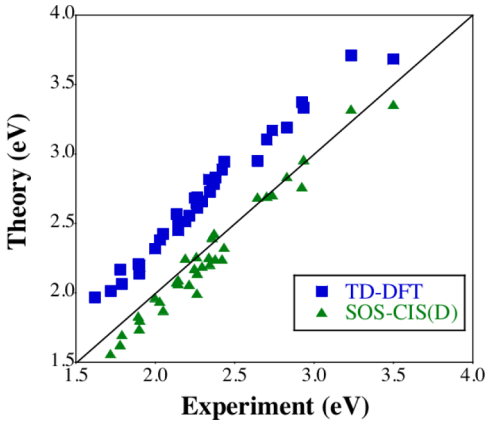

Figure 2. Comparison of the TD-DFT, SOS-CIS(D), and experimental E^{AFCP} values for the BODIPY dyes displayed in Scheme 3.

dyes shown in Scheme 2 is given in Table 4, and the 0−0 energies obtained with TD-DFT-M06-2X, CIS(D), and SOS-CIS(D) are available in the SI. We have not reported SD and R^2 values in Table 4 because they would be completely insignificant for such a small set of molecules. For the three selected approaches, the computed 0−0 energies systematically exceed their experimental counterparts. In the case of TD-DFT, the deviation is as large as 0.4 eV, whereas the two pertubative approaches again provide more accurate results. Indeed, the range of deviations is 0.185−0.137 eV for CIS(D) and 0.077−0.037 eV for SOS-CIS(D). Therefore, the MSE and MAE for TD-DFT are reduced by almost 1 order of magnitude when SOS-CIS(D) corrections are included, confirming the success of the proposed protocol.

Figure 6 shows the M06-2X density difference plots computed for the four aza-BODIPY dyes. Adding a *tert*-butyl (*t*-Bu) electron donor at both extremities (going from **Az.1** to **Az.2**) induces very small bathochromic shifts (+3 nm for the absorption and +4 nm for the emission). These computed values perfectly match experiment (+3 and +3 nm, respectively) and are also consistent with the similar topologies of the density difference plots shown in Figure 6. Indeed, the *t*-Bu groups do not tune the geometry of the core of the molecule or play any direct role in the optical transition. The ESs are localized only on the aza-BODIPY core and on the lateral phenyl rings. **Az.1** and **Az.2** also present similar CT parameters (Table 5). Changing the *t*-Bu groups (**Az.2**) to an electron-withdrawing unit (CF_3 in **Az.3** or NO_2 in **Az.4**) might have been expected to yield much more significant effects. However, this was not the case, as even the strong nitro groups participate only marginally in the ES (Figure 6). This is consistent with the very small auxochromic effects measured in ref 70 and reproduced by SOS-CIS(D).

Table 3. CT Distances (d^{CT}, in Å), Transferred Charges (q^{CT}, in *e*), and CT Dipole Moments (μ^{CT}, in D) for the Molecules Shown in Figure 3

dye	d^{CT}	q^{CT}	μ^{CT}
Bo.9	1.81	0.40	3.38
Bo.10	1.28	0.38	2.35
Bo.11	1.10	0.40	2.14
Bo.12	1.43	0.41	2.88

Finally, in Figure 7 we report theoretical absorption and emission band shapes calculated for the aza-BODIPY dyes shown in Scheme 2. The four dyes present notable vibronic structures, and here again theory very nicely reproduces the experimental band topologies (see ref 70). The contributions of individual components of **Az.1** are also given in the right panel of Figure 7, while the corresponding spectra for the other dyes are available in the SI. For **Az.1**, we can distinguish major vibrational contributions explaining the emergence of the second band. These vibrational modes present energies of 1467 and 1470 cm^{-1} for the GS (hence the emission spectrum) and the ES (hence the absorption spectrum), respectively. Movies of these modes are available in the SI. They can be characterized as C−C and C−N stretching in the aza-BODIPY core, but they do not involve the BF_2 moiety or the side phenyl rings.

4. CONCLUSIONS

We have simulated the spectra of more than 50 fluoroborate derivatives of the (aza-)BODIPY family using an approach that includes structural relaxation, solvent, and vibrational effects at the TD-DFT level whereas the transition energies are obtained with the (SOS)-CIS(D) approach. Such a hybrid approach allowed us to obtain, for the first time, excited-state properties that are both accurate and directly comparable to the experimental measurements for this key class of compounds. Such success could not be attained by considering the methods separately. The mean absolute deviations of the 0−0 energies provided by TD-DFT are indeed cut by a factor of ca. 5 upon the addition of SOS-CIS(D) corrections (to values below 0.1 eV), while at the same time the very large theory/experiment correlation coefficients typical of TD-DFT are preserved. The SOS-CIS(D)//TD-DFT protocol presented here is computationally efficient and can be straightforwardly applied to large set of real-life dyes, and it will be particularly interesting to circumvent the *cyanine problem* of TD-DFT. In addition, we found (1) that SOS-CIS(D) is significantly more accurate than CIS(D) for the treated molecules; (2) that the vibronic effects

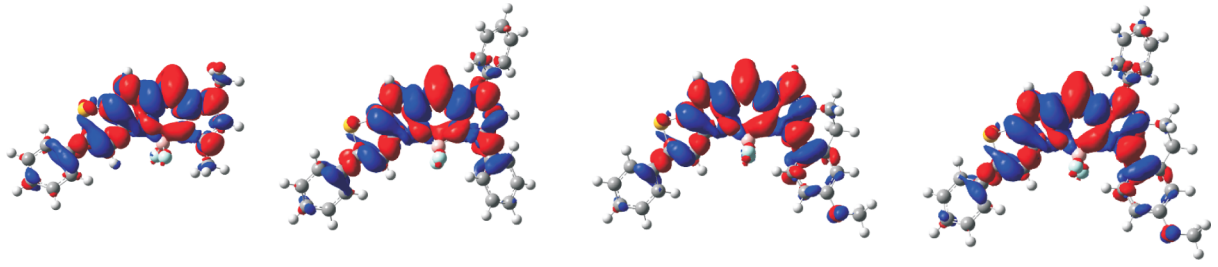

Figure 3. PCM-TD-M06-2X/6-31G(d) density difference plots (from left to right) for the BODIPY dyes **Bo.9**, **Bo.10**, **Bo.11**, and **Bo.12**. The blue (red) zones indicate density decreases (increases) upon transition. The selected contour threshold is 0.0004 au.

dx.doi.org/10.1021/ct500655k | J. Chem. Theory Comput. 2014, 10, 4574−4582

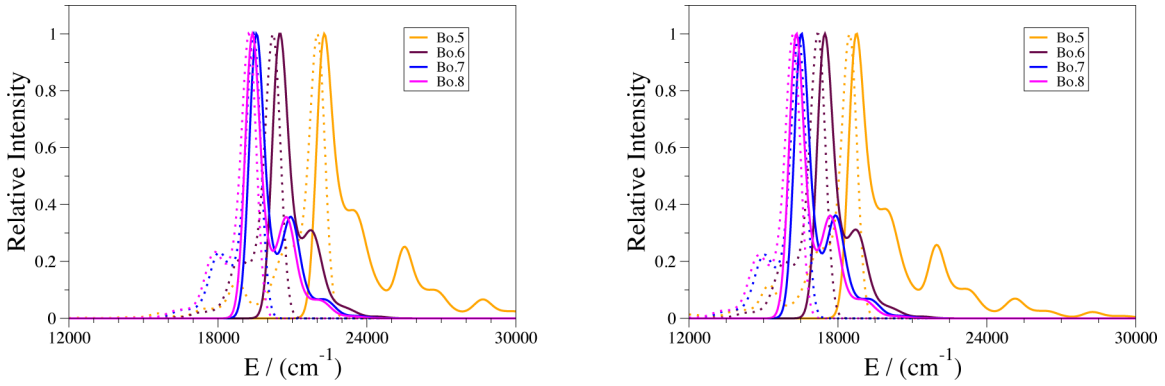

Figure 4. Absorption (solid lines) and emission (dashed lines) TD-DFT (left) and SOS-CIS(D) (right) spectra for BODIPY dyes **Bo.5**, **Bo.6**, **Bo.7**, and **Bo.8**. The vibrational structures were obtained through TD-DFT in both cases (see the text).

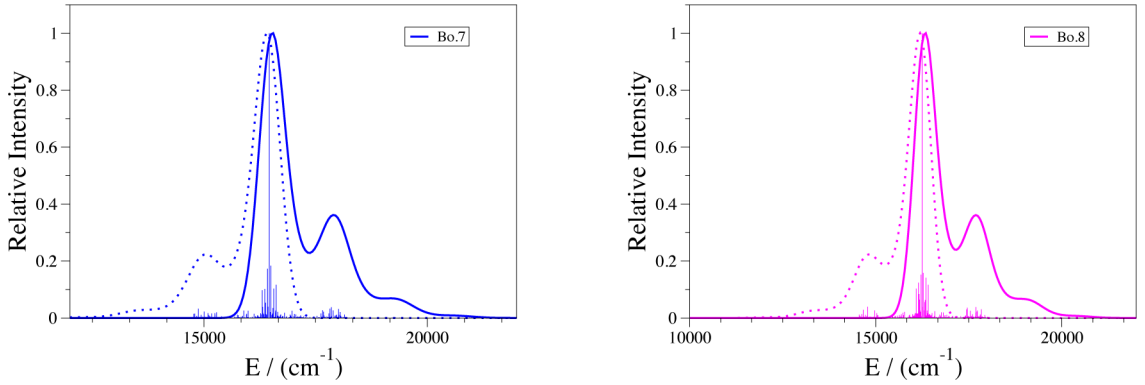

Figure 5. Absorption (solid lines) and emission (dashed lines) spectra of **Bo.7** (left) and **Bo.8** (right) together with the contribution of individual vibrations (represented as sticks). See the caption of Figure 4 for more details.

Table 4. Statistical Analysis for the Aza-BODIPY Dyes Shown in Scheme 2 Obtained with the PCM-TDDFT, CIS(D), and SOS-CIS(D) Approaches (All Values Are Given in eV)

method	MSE	MAE	Max(+)	Max(−)
E_{BE}^{AFCP}(TD, SS, neq)	0.425	0.425	0.457	0.407
E_{BE}^{AFCP}(CIS(D), SS, neq)	0.161	0.161	0.185	0.137
E_{BE}^{AFCP}(SOS-CIS(D), SS, neq)	0.056	0.056	0.077	0.037

Table 5. CT Parameters for the Four Aza-BODIPY Dyes[a]

dye	d^{CT}	q^{CT}	μ^{CT}
Az.1	0.40	0.50	0.97
Az.2	0.50	0.50	1.21
Az.3	0.28	0.49	0.64
Az.4	0.07	0.50	0.17

[a]See the caption of Table 3 for more details.

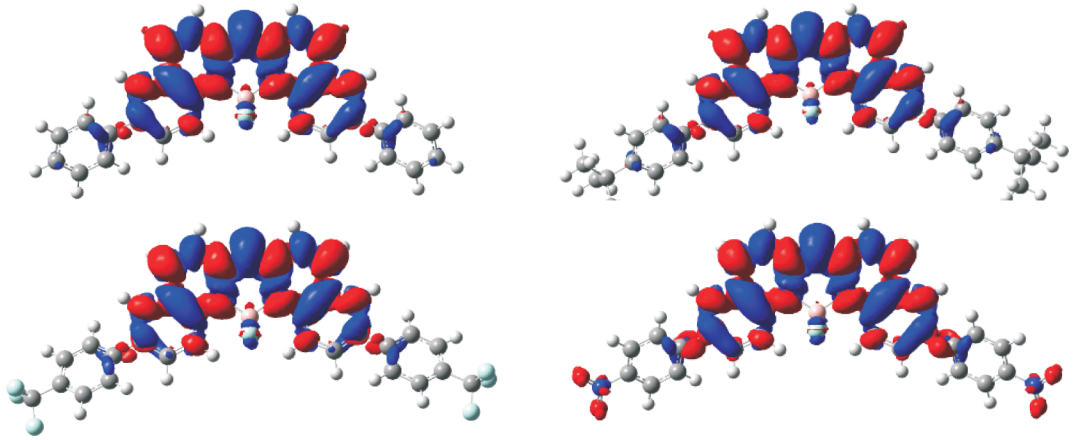

Figure 6. PCM-TD-M06-2X/6-31G(d) density difference plots for **Az.1** (top left), **Az.2** (top right), **Az.3** (bottom left), and **Az.4** (bottom right). See the caption of Figure 3 for more details.

dx.doi.org/10.1021/ct500655k | J. Chem. Theory Comput. 2014, 10, 4574−4582

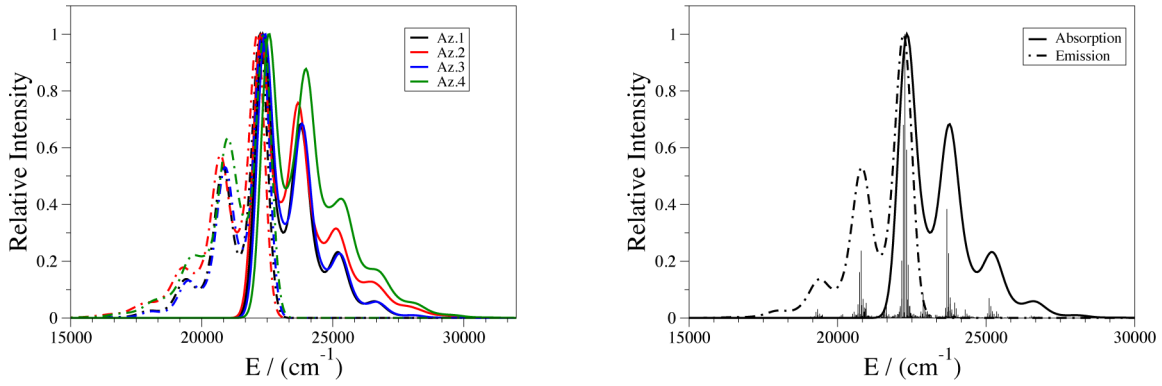

Figure 7. Absorption (solid lines) and emission (dashed lines) spectra of aza-BODIPY dyes **Az.1**, **Az.2**, **Az.3**, and **Az.4** (left) and individual vibronic contributions (given as sticks) for **Az.1** (right). See the caption of Figure 4 for more details.

obtained with TD-DFT match experiment; and (3) that for the BODIPY dyes the red shifts are not systematically related to enhanced CT.

■ ASSOCIATED CONTENT

Supporting Information

Detailed protocol for the calculation of AFCP energies with TD-DFT, list of solvents, experimental absorption and emission values, 0−0 energies with different solvent models for all compounds, extra vibronic analysis, and movies of vibrational modes (AVI). This material is available free of charge via the Internet at http://pubs.acs.org.

■ AUTHOR INFORMATION

Corresponding Authors

*E-mail: Adele.Laurent@univ-nantes.fr.
*E-mail: Boris.leguennic@univ-rennes1.fr.
*E-mail: Denis.Jacquemin@univ-nantes.fr.

Notes

The authors declare no competing financial interest.

■ ACKNOWLEDGMENTS

S.C. thanks the European Research Council (ERC) (Marches - 278845) for her Ph.D. grant. D.J. acknowledges the ERC and the Région des Pays de la Loire for financial support in the framework of a Starting Grant (Marches - 278845) and a Recrutement sur Poste Stratégique, respectively. This research used resources of (1) the GENCI-CINES/IDRIS (Grants c2013085117 and x2013080649), (2) Centre de Calcul Intensif des Pays de Loire (CCIPL), and (3) a local Troy cluster.

■ REFERENCES

(1) Erten-Ela, S.; Yilmaz, M. D.; Icli, B.; Dede, Y.; Icli, S.; Akkaya, E. U. *Org. Lett.* **2008**, *10*, 3299−3302.
(2) Rousseau, T.; Cravino, A.; Bura, T.; Ulrich, G.; Ziessel, R.; Roncali, J. *Chem. Commun.* **2009**, 1673−1675.
(3) Whited, M. T.; Djurovich, P. I.; Roberts, S. T.; Durrell, A. C.; Schlenker, C. W.; Bradforth, S. E.; Thompson, M. E. *J. Am. Chem. Soc.* **2011**, *133*, 88−96.
(4) Flavin, K.; Lawrence, K.; Bartelmess, J.; Tasior, M.; Navio, C.; Bittencourt, C.; O'Shea, D. F.; Guldi, D. M.; Giordani, S. *ACS Nano* **2011**, *5*, 1198−1206.
(5) Lehl, J.; Nierengarten, J. F.; Harriman, A.; Bura, T.; Ziessel, R. *J. Am. Chem. Soc.* **2012**, *134*, 988−998.
(6) Zheng, Q.; Xu, G.; Prasad, P. N. *Chem.—Eur. J.* **2008**, *14*, 5812−5819.
(7) Bouit, P.-A.; Kamada, K.; Feneyrou, P.; Berginc, G.; Toupet, L.; Maury, O.; Andraud, C. *Adv. Mater.* **2009**, *21*, 1151−1154.
(8) Didier, P.; Ulrich, G.; Mély, Y.; Ziessel, R. *Org. Biomol. Chem.* **2009**, *7*, 3639−3642.
(9) Coskun, A.; Yilmaz, M.; Akkaya, E. U. *Org. Lett.* **2007**, *9*, 607−609.
(10) Murtagh, J.; Frimannsson, D. O.; O'Shea, D. F. *Org. Lett.* **2009**, *11*, 5386−5389.
(11) Han, J.; Loudet, A.; Barhoumi, R.; Burghardt, R. C.; Burgess, K. *J. Am. Chem. Soc.* **2009**, *131*, 1642−1643.
(12) Shi, W. J.; Liu, J. Y.; Ng, D. K. P. *Chem.—Asian J.* **2012**, *7*, 196−200.
(13) Killoran, J.; Allen, L.; Gallagher, J. F.; Gallagher, W. M.; O'Shea, D. F. *Chem. Commun.* **2002**, 1862−1863.
(14) Byrne, A. T.; O'Connor, A. E.; Hall, M.; Murtagh, J.; O'Neill, K.; Curran, K. M.; Mongrain, K.; Rousseau, J. A.; Lecomte, R.; McGee, S.; Callanan, J. J.; O'Shea, D. F.; Gallagher, W. M. *Br. J. Cancer.* **2009**, *101*, 1565−1573.
(15) Adarsh, N.; Avirah, R. R.; Ramaiah, D. *Org. Lett.* **2010**, *12*, 5720−5723.
(16) Loudet, A.; Burgess, K. *Chem. Rev.* **2007**, *107*, 4891−4932.
(17) Ulrich, G.; Ziessel, R.; Harriman, A. *Angew. Chem., Int. Ed.* **2008**, *47*, 1184−1201.
(18) Frath, D.; Massue, J.; Ulrich, G.; Ziessel, R. *Angew. Chem., Int. Ed.* **2014**, *53*, 2290−2310.
(19) Grimme, S.; Neese, F. *J. Chem. Phys.* **2007**, *127*, No. 154116.
(20) Jacquemin, D.; Zhao, Y.; Valero, R.; Adamo, C.; Ciofini, I.; Truhlar, D. G. *J. Chem. Theory Comput.* **2012**, *8*, 1255−1259.
(21) Moore, B., II; Autschbach, J. *J. Chem. Theory Comput.* **2013**, *9*, 4991−5003.
(22) Zhekova, H.; Krykunov, M.; Autschbach, J.; Ziegler, T. *J. Chem. Theory Comput.* **2014**, *10*, 3299−3307.
(23) Quartarolo, A. D.; Russo, N.; Sicilia, E. *Chem.—Eur. J.* **2006**, *12*, 6797−6803.
(24) Gresser, R.; Hartmann, H.; Wrackmeyer, M.; Leo, K.; Riede, M. *Tetrahedron* **2011**, *67*, 7148−7155.
(25) Le Guennic, B.; Maury, O.; Jacquemin, D. *Phys. Chem. Chem. Phys.* **2012**, *14*, 157−164.
(26) Bakalova, S.; Mendicuti, F.; Castano, O.; Kaneti, J. *Chem. Phys. Lett.* **2009**, *478*, 206−210.
(27) Yoshino, J.; Kambe, A. F. T.; Itoi, H.; Kano, N.; Kawashima, T.; Ito, Y.; Asashima, M. *Chem.—Eur. J.* **2010**, *16*, 5026−5035.
(28) Lazarides, T.; McCormick, T. M.; Wilson, K. C.; Lee, S.; McCamant, D. W.; Eisenberg, R. *J. Am. Chem. Soc.* **2011**, *133*, 350−364.
(29) Bellier, Q.; Pegaz, S.; Aronica, C.; Le Guennic, B.; Andraud, C.; Maury, O. *Org. Lett.* **2011**, *13*, 22−25.
(30) Guo, H.; Jing, Y.; Yuan, X.; Ji, S.; Zhao, J.; Lib, X.; Kan, Y. *Org. Biomol. Chem.* **2011**, *9*, 3844−3853.
(31) Awuah, S. G.; Polreis, J.; Biradar, V.; You, Y. *Org. Lett.* **2011**, *13*, 3884−3887.

(32) Nakamura, M.; Tahara, T.; Takahashi, K.; Nagata, T.; Uoyama, H.; Kuzuhara, D.; Mori, S.; Okujima, T.; Yamada, H.; Uno, H. *Org. Biomol. Chem.* **2012**, *10*, 6840−6849.
(33) Gai, L.; Lu, H.; Zou, B.; Lai, G.; Shen, Z.; Li, Z. *RSC Adv.* **2012**, *2*, 8840−8846.
(34) Khan, T. K.; Shaikh, M. S.; Ravikanth, M. *Dyes Pigm.* **2012**, *94*, 66−73.
(35) Ni, Y.; Zeng, W.; Huang, K. W.; Wu, J. *Chem. Commun.* **2013**, *49*, 1217−1219.
(36) Choi, S.; Bouffard, J.; Kim, Y. *Chem. Sci.* **2014**, *5*, 751−755.
(37) Alberto, M. E.; De Simone, B. C.; Mazzone, G.; Quartarolo, A. D.; Russo, N. *J. Chem. Theory Comput.* **2014**, DOI: 10.1021/ct500426h.
(38) Chibani, S.; Le Guennic, B.; Charaf-Eddin, A.; Maury, O.; Andraud, C.; Jacquemin, D. *J. Chem. Theory Comput.* **2012**, *8*, 3303−3313.
(39) Chibani, S.; Le Guennic, B.; Charaf-Eddin, A.; Laurent, A. D.; Jacquemin, D. *Chem. Sci.* **2013**, *4*, 1950−1963.
(40) Runge, E.; Gross, E. K. U. *Phys. Rev. Lett.* **1984**, *52*, 997−1000.
(41) Send, R.; Valsson, O.; Filippi, C. *J. Chem. Theory Comput.* **2011**, *7*, 444−455.
(42) Boulanger, P.; Jacquemin, D.; Duchemin, I.; Blase, X. *J. Chem. Theory Comput.* **2014**, *10*, 1212−1218.
(43) Head-Gordon, M.; Rico, R. J.; Oumi, M.; Lee, T. J. *Chem. Phys. Lett.* **1994**, *219*, 21−29.
(44) Head-Gordon, M.; Maurice, D.; Oumi, M. *Chem. Phys. Lett.* **1995**, *246*, 114−121.
(45) Goerigk, L.; Moellmann, J.; Grimme, S. *Phys. Chem. Chem. Phys.* **2009**, *11*, 4611−4620.
(46) Grimme, S.; Izgorodina, E. I. *Chem. Phys.* **2004**, *305*, 223−230.
(47) Oumi, M.; Maurice, D.; Head-Gordon, M. *Spectrochim. Acta, Part A* **1999**, *55*, 525−537.
(48) Lee, T. J.; Parthiban, S.; Head-Gordon, M. *Spectrochim. Acta, Part A* **1999**, *55*, 561−574.
(49) Lochan, R. C.; Shao, Y.; Head-Gordon, M. *J. Chem. Theory Comput.* **2007**, *3*, 988−1003.
(50) Rhee, Y. M.; Head-Gordon, M. *J. Phys. Chem. A* **2007**, *111*, 5314−5326.
(51) Rhee, Y. M.; Casanova, D.; Head-Gordon, M. *J. Chem. Theory Comput.* **2009**, *5*, 1224−1236.
(52) All of the ES structures were optimized using the TD-DFT approach.
(53) Goerigk, L.; Grimme, S. *J. Chem. Phys.* **2010**, *132*, No. 184103.
(54) Winter, N. O. C.; Hättig, C. *J. Chem. Phys.* **2011**, *134*, No. 184101.
(55) Winter, N. O. C.; Graf, N. K.; Leutwyler, S.; Hättig, C. *Phys. Chem. Chem. Phys.* **2013**, *15*, 6623−6630.
(56) Frisch, M. J.; Trucks, G. W.; Schlegel, H. B.; Scuseria, G. E.; Robb, M. A.; Cheeseman, J. R.; Scalmani, G.; Barone, V.; Mennucci, B.; Petersson, G. A.; Nakatsuji, H.; Caricato, M.; Li, X.; Hratchian, H. P.; Izmaylov, A. F.; Bloino, J.; Zheng, G.; Sonnenberg, J. L.; Hada, M.; Ehara, M.; Toyota, K.; Fukuda, R.; Hasegawa, J.; Ishida, M.; Nakajima, T.; Honda, Y.; Kitao, O.; Nakai, H.; Vreven, T.; Montgomery, J. A., Jr.; Peralta, J. E.; Ogliaro, F.; Bearpark, M.; Heyd, J. J.; Brothers, E.; Kudin, K. N.; Staroverov, V. N.; Kobayashi, R.; Normand, J.; Raghavachari, K.; Rendell, A.; Burant, J. C.; Iyengar, S. S.; Tomasi, J.; Cossi, M.; Rega, N.; Millam, J. M.; Klene, M.; Knox, J. E.; Cross, J. B.; Bakken, V.; Adamo, C.; Jaramillo, J.; Gomperts, R.; Stratmann, R. E.; Yazyev, O.; Austin, A. J.; Cammi, R.; Pomelli, C.; Ochterski, J. W.; Martin, R. L.; Morokuma, K.; Zakrzewski, V. G.; Voth, G. A.; Salvador, P.; Dannenberg, J. J.; Dapprich, S.; Daniels, A. D.; Farkas, Ö.; Foresman, J. B.; Ortiz, J. V.; Cioslowski, J.; Fox, D. J. *Gaussian 09*, revision D.01; Gaussian, Inc.: Wallingford, CT, 2009.
(57) Zhao, Y.; Truhlar, D. G. *Theor. Chem. Acc.* **2008**, *120*, 215−241.
(58) Improta, R.; Scalmani, G.; Frisch, M. J.; Barone, V. *J. Chem. Phys.* **2007**, *127*, No. 074504.
(59) Tomasi, J.; Mennucci, B.; Cammi, R. *Chem. Rev.* **2005**, *105*, 2999−3094.
(60) Shao, Y.; Fusti Molnar, L.; Jung, Y.; Kussmann, J.; Ochsenfeld, C.; Brown, S. T.; Gilbert, A. T. B.; Slipchenko, L. V.; Levchenko, S. V.; O'Neill, D. P.; DiStasio, R. A., Jr.; Lochan, R. C.; Wang, T.; Beran, G. J. O.; Besley, N. A.; Herbert, J. M.; Lin, C. Y.; Van Voorhis, T.; Chien, S. H.; Sodt, A.; Steele, R. P.; Rassolov, V. A.; Maslen, P. E.; Korambath, P. P.; Adamson, R. D.; Austin, B.; Baker, J.; Bird, E. F. C.; Daschel, H.; Doerksen, R. J.; Dreuw, A.; Dunietz, B. D.; Dutoi, A. D.; Furlani, T. R.; Gwaltney, S. R.; Heyden, A.; Hirata, S.; Hsu, C.-P.; Kedziora, G.; Khalliulin, R. Z.; Klunziger, P.; Lee, A. M; Lee, M. S; Liang, W.; Lotan, I.; Nair, N.; Peters, B.; Proynov, E. I.; Pieniazek, P. A.; Rhee, Y. M.; Ritchie, J.; Rosta, E.; Sherrill, C. D.; Simmonett, A. C.; Subotnik, J. E.; Woodcock, H. L., III; Zhang, W.; Bell, A. T.; Chakraborty, A. K.; Chipman, D. M.; Keil, F. J.; Warshel, A.; Hehre, W. J.; Schaefer, H. F., III; Kong, J.; Krylov, A. I.; Gill, P. M. W.; Head-Gordon, M. *Phys. Chem. Chem. Phys.* **2006**, *8*, 3172−3191.
(61) Santoro, F.; Improta, R.; Lami, A.; Bloino, J.; Barone, V. *J. Chem. Phys.* **2007**, *126*, No. 084509.
(62) Santoro, F.; Improta, R.; Lami, A.; Bloino, J.; Barone, V. *J. Chem. Phys.* **2007**, *126*, No. 184102.
(63) Santoro, F.; Lami, A.; Improta, R.; Bloino, J.; Barone, V. *J. Chem. Phys.* **2008**, *128*, No. 224311.
(64) Avila Ferrer, F. J.; Cerezo, J.; Stendardo, E.; Improta, R.; Santoro, F. *J. Chem. Theory Comput.* **2013**, *9*, 2072−2082.
(65) Jacquemin, D.; Planchat, A.; Adamo, C.; Benedetta, M. *J. Chem. Theory Comput.* **2012**, *8*, 2359−2372.
(66) Laurent, A. D.; Jacquemin, D. *Int. J. Quantum Chem.* **2013**, *113*, 2019−2039.
(67) Le Bahers, T.; Adamo, C.; Ciofini, I. *J. Chem. Theory Comput.* **2011**, *7*, 2498−2506.
(68) Jacquemin, D.; Le Bahers, T.; Adamo, C.; Ciofini, I. *Phys. Chem. Chem. Phys.* **2012**, *14*, 5383−5388. Code available at Université de Nantes, http://www.sciences.univ-nantes.fr/CEISAM/erc/marches/ (accessed May 1, 2014)..
(69) Jiang, X. D.; Zhang, H.; Zhang, Y.; Zhao, W. *Tetrahderon* **2012**, *68*, 9795−9801.
(70) Wang, D.; Liu, R.; Chen, C.; Wang, S.; Chang, J.; Wu, C.; Zhu, H. *Dyes Pigm.* **2013**, *99*, 240−249.